ELSEVIER

Global and Planetary Change 18 (1998) 113–128

GLOBAL AND PLANETARY CHANGE

Climate extremes in Loess of China coupled with the strength of deep-water formation in the North Atlantic

Zhengtang Guo [a,*], Tungsheng Liu [a], Nicolas Fedoroff [b], Lanying Wei [a], Zhongli Ding [a], Naiqin Wu [a], Huoyuan Lu [a], Wenying Jiang [a], Zhisheng An [c]

[a] *Institute of Geology, Chinese Academy of Sciences, PO Box 9825, Beijing 100029, China*
[b] *DEMOS, Ager, Institut National Agronomique Paris-Grignon, Thiverval-Grignon 78850, France*
[c] *Xian Laboratory of Loess and Quaternary Geology, Chinese Academy of Sciences, PO Box 17, Xian 710054, China*

Received 6 May 1997; accepted 29 September 1997

Abstract

The loess-paleosol sequences of the last 1.2 Ma in China have recorded two kinds of climate extremes: the strongly developed S4, S5-1 and S5-3 soils (corresponding to the marine $\delta^{18}O$ stages 11, 13, and 15, respectively) as evidence of three episodes of great warmth and two coarse-grained loess units (L9 and L15, corresponding to the marine $\delta^{18}O$ stages 22, 23, 24 and 38, respectively) which indicate severest glacial conditions. The climatic and geographical significance of these events are still unclear, and their cause remains a puzzle.

Paleopedological, geochemical and magnetic susceptibility data from three loess sections (Xifeng, Changwu and Weinan) suggest that the S4, S5-1 and S5-3 soils were formed under sub-tropical semi-humid climates with a tentatively estimated mean annual temperature (MAT) of at least 4–6°C higher and a mean annual precipitation (MAP) of 200–300 mm higher than for the present-day, indicating a much strengthened summer monsoon. The annual rainfall was particularly accentuated for the southern-most part of the Loess Plateau, suggesting that the monsoon rain belt (the contact of the monsoonal northward warm-humid air mass with the dry-cold southward one) might have stood at the southern part of the Plateau for a relatively long period each year. The loess units L9 and L15 were deposited under semi-desertic environments with a tentatively estimated MAT and MAP of only about 1.5–3°C and 150–250 mm, indicating a much strengthened winter monsoon, and that the summer monsoon front could rarely penetrate into the Loess Plateau region.

Correlation with marine carbon isotope records suggests that these climate extremes have large regional, even global, significance rather than being local phenomena in China. They match the periods with greatest/smallest Atlantic–Pacific $\delta^{13}C$ gradients, respectively, indicating their relationships with the strength of Deep Water (NADW) production in the North Atlantic. These results suggest that the monsoon climate in the Loess Plateau region was significantly linked with the North Atlantic thermohaline circulation on timescales of 10^4 years.

Keywords: loess; paleosol; monsoons; paleoclimate; North Atlantic Deep Water

* Corresponding author. Tel.: +8610620008110. Fax: +861062052184. E-mail: ztguo@mimi.cnc.ac.cn

0921-8181/98/$19.00
PII S0921-8181(98)00010-1

1. Introduction

The alternation of loess and paleosols in the Loess Plateau (Fig. 1) of China provides an apparently continuous record of continental climate over the past 2.5 Ma (Liu, 1985; Kukla and An, 1989; An et al., 1991a,b). Its stratigraphy can be generally correlated with that of the marine $\delta^{18}O$ record (Liu, 1985; Liu and Yuan, 1987; Kukla, 1987; Rutter et al., 1991), and the correlation pattern for the last 1.2 Ma, shown in Fig. 2, is commonly accepted (Kukla, 1987; Rutter et al., 1991), and is confirmed by the aeolian dust record in the North Pacific (Hovan et al., 1989), which is a direct link between the China loess and marine $\delta^{18}O$ records. A complete sequence of the last 2.5 Ma has recorded at least 56 soil-forming intervals (Guo et al., 1996) and the major interglacial soils (monocyclic or polycyclic) and the interbedded loess units of the last 1.2 Ma are labeled as S0, L1, S1, L2, S2, ..., S14, L15 from the top to the bottom according to Liu (1985). The loess L1 is also ascribed as Malan Loess and the sequence from S1 to L15 as Lishi Loess. The S5 soil unit consists of three sub-units separated by clear interbedded loess layers, labeled S5-1, S5-2 and S5-3, respectively (Fig. 2).

The Loess Plateau is located in the East Asian monsoon zone (Zhang and Lin, 1987). In summer, the region is under the control of the warm-humid southeast summer monsoon of tropical/subtropical origin, leading to abundant precipitation. In winter, the cold-dry northwest winter monsoon of sub-arctic origin prevails across the region. The climate is thus highly seasonal with a much warmer summer and much cooler winter than for the non-monsoon regions of the same latitudes. In spring, the summer monsoon begins to penetrate progressively inland, and its northern front constitutes an important rain belt. From early June to early July of each year, this belt usually reaches and is detained in the Yangtz–Huaihe River basin (between 26–34° N in eastern China), resulting in a long and continuous rainy season (the so-called 'Meiyu belt' or 'plum rain belt'). Then, the front penetrates into northern China, including the Loess Plateau, due to the strengthening of the monsoon, where most of the annual rainfall is

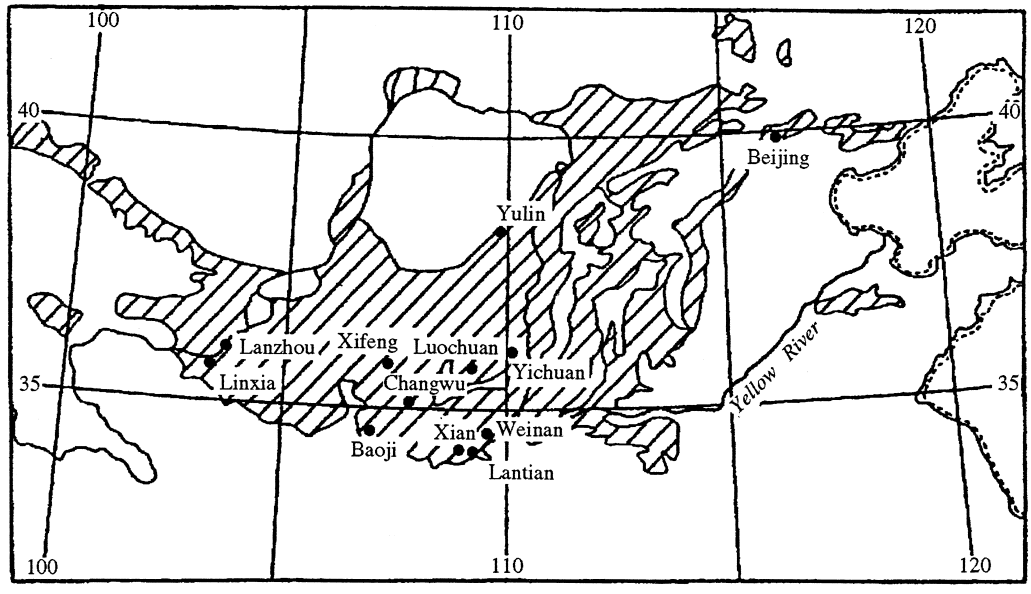

Fig. 1. Sketch map showing the Loess Plateau and location of the studied sites.

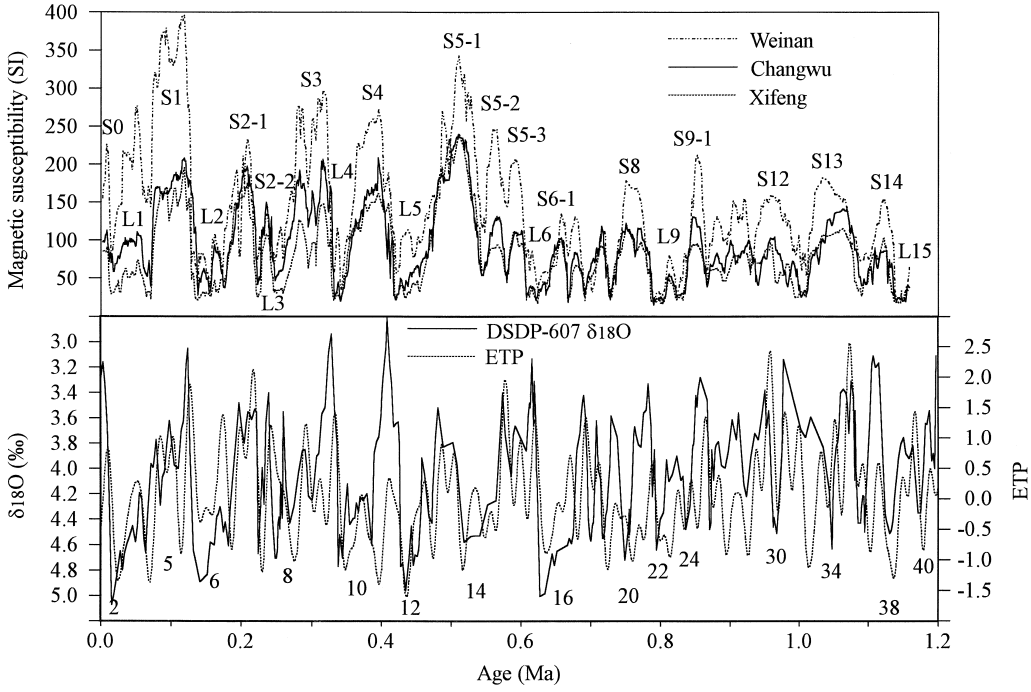

Fig. 2. Correlation of the loess–paleosol sequences in Xifeng, Changwu and Weinan with marine δ^{18}O record and orbital variations. The Xifeng timeseries of magnetic susceptibility (Xifeng I) is from Kukla et al. (1990), which is dated by a susceptibility age model using the magnetostratigraphic boundaries as age controllers. The timescales for Changwu and Weinan were obtained by correlation with the Xifeng susceptibility curve. δ^{18}O timeseries of DSDP Site 607 is from Ruddiman et al. (1989). The oxygen isotope stages are labeled. The slight dislocation between the susceptibility and marine δ^{18}O timeseries for some soil and loess units is due to the difference in the timescales used. Data of the orbital parameters (eccentricity, obliquity and precession) are from Berger and Loutre (1991). The ETP is assumed to reflect the insolation changes in the northern hemisphere (Clemens et al., 1991), and is obtained by adding the normalized eccentricity (E), obliquity (T) and inverted precession (P).

concentrated in July, August and September (Zhang and Lin, 1987). As the initiation of monsoon climate in Asia can be traced back to the pre-Quaternary era (Ruddiman and Kutzbach, 1989), the loess–soil sequence is commonly interpreted as an indication of alternate waxing and waning of the summer and winter paleomonsoons; the soil-forming periods correspond to strengthened summer monsoon, and loess deposition corresponds to strengthened winter monsoon (An et al., 1991a,b; Liu and Ding, 1993; Liu et al., 1995).

Since the stratigraphy of the loess–soil sequences correlates well with marine δ^{18}O records, it is considered that loess deposition was primarily related to the variations in global ice-volume (Liu and Ding, 1993; Guo et al., 1994; Liu et al., 1995). Changes in the northern summer insolation have also been invoked to explain the variability of the monsoon climate over the last climatic cycle (An et al., 1991a; Guo et al., 1994; Liu et al., 1995). However, a number of differences exist between the loess–soil sequence and marine δ^{18}O records (Kukla, 1987; Guo, 1990; Liu and Ding, 1993; Guo et al., 1994, 1996a; Liu et al., 1995), among which the strongly developed soil units S4, S5-1, S5-3 and the coarse-grained loess units L9 and L15, also ascribed as 'sandy loess', have presented particularly puzzling issues (Liu, 1985; Kukla, 1987; Bronger and Heinkele, 1989; Guo, 1990; Liu and Ding, 1993). These units are widely used as stratigraphic markers (Liu, 1985) because of their specific field morphological characteristics. The three soils, especially the S5-1, represent the most strongly developed soils (An and Wei, 1980; Bronger and Heinkele, 1989;

Guo, 1990) and thus mark the periods of greatest warmth in the east Asian monsoon zone, while the sandy loess L9 and L15 represent the severest glacial periods (Liu, 1985; Guo, 1990; Guo et al., 1993b). The cause of these climate extremes remains unclear, and their geographical significance is still a matter of debate (Bronger and Heinkele, 1989; Billard, 1993). Moreover, interpretation of the climatic amplitudes in loess–soil sequences older than the last climatic cycle are still qualitative and sometimes controversial and, therefore, need further studies.

Based on the paleopedological, geochemical and magnetic susceptibility data from three selected sites under different modern climatic conditions, this paper aims: (1) to address the environmental conditions reflected by these particular soil and loess units; (2) to interpret the latitudinal amplitudes of the climatic zones indicated by these loess and paleosols, compared with the present-day situation; and (3) to address the geographical significance of these climatic extremes and the potential forcing factors and mechanisms.

2. General setting and methods

Three loess sections (Xifeng, Changwu and Weinan) have been selected along a northwest–southeast direction (Fig. 1). This transect has the steepest climatic gradients in the Loess Plateau region because of the interaction of the southeast summer monsoon and the northwest winter monsoon. The Xifeng and Weinan sections are type sections, having been the focus of a number of studies (Liu et al., 1987; Kukla, 1987; Guo, 1990; Guo et al., 1991). The modern mean annual temperature (MAT) and precipitation (MAP) in Xifeng are 8.3°C and 560 mm, respectively. The Weinan site is located at the southern-most part of the Loess Plateau with a MAT of 13°C and a MAP of 650 mm. The

Table 1
Munsell color and micromorphological features of the paleosols in Weinan and Xifeng

Soil unit	Weinan					Xifeng				
	Munsell code	Detrital CaCO3 (%)	Clay coating (%)	Fe–Mn feature (%)	Fine fraction (%)	Munsell code	Detrital $CaCO_3$ (%)	Clay coating (%)	Fe–Mn feature (%)	Fine fraction (%)
S0	7.5 YR 4/6	0	1	2	35	10 YR 4/3	1	0	0	15
S1	5 YR 4/6	0	6	3	40	7.5 YR 5/4	0	0.5	0	20
S2-1	5 YR 4/8	0	5	2	40	7.5 YR 5/4	0	0	0	20
S2-2	7.5 YR 5/8	0.5	0	0	20	10 YR 8/4	3	0	0	10
S3	5 YR 5/8	0	0.5	0.5	45	7.5 YR 5/4	2	0	0	15
S4	2.5 YR 4/6	0	8	3	45	5 YR 4/6	0	0.5	0	25
S5-1	2.5 YR 4/8	0	13	2	50	5 YR 4/6	0	3	0.5	30
S5-2	5 YR 4/8	0	3	3.5	40	7.5 YR 5/6	0	0	0	20
S5-3	5 YR 4/6	0	8	3	45	5 YR 4/4	0	2	0	25
S6-1	5 YR 4/4	0	6	0.5	40	7.5 YR 5/6	0	0	0	20
S6-2	7.5 YR 4/6	0.5	0	1.5	20	7.5 YR 7/4	3	0	0	10
S7	5 YR 3/6	0	5	3	35	7.5 YR 6/4	1	0	0	15
S8	5 YR 4/6	0	6	1.5	40	7.5 YR 5/4	0	0	0	18
S9-1	7.5 YR 4/6	0	2	0.5	30	7.5 YR 6/4	1	0	0	15
S9-2	7.5 YR 5/6	0	0	3	20	7.5 YR 6/4	2	0	0	18
S10	7.5 YR 4/6	0	0	0	20	7.5 YR 7/4	2	0	0	15
S11	5 YR 4/6	0	0	1	15	7.5 YR 6/4	2	0	0	15
S12-1	5 YR 4/8	0	0	1	25	7.5 YR 5/4	1	0	0	15
S12-2	7.5 YR 5/8	0.5	0	0	20	7.5 YR 7/4	2	0	0	12
S13	5 YR 4/8	0	4	1.5	40	5 YR 5/6	0	0	0	20
S14	7.5 YR 5/6	0	0	0	25	7.5 YR 7/4	1	0	0	15

The listed features correspond to the soil horizon with the maximum value of magnetic susceptibility.

Changwu section is a new site (Fig. 1), situated between Xifeng and Weinan, with a MAT of 9.1°C and a MAP of 590 mm.

Stratigraphic correlation of the three sections was made according to widely used stratigraphic markers. These are the top dark Holocene soil S0, the last interglacial soil S1 (corresponding to marine $\delta^{18}O$ stage 5), the strongly developed and rubified S4 and S5 soils with the latter subdivided into three soils with thin interbedded loess layers, and the two sandy loess L9 and L15 (Fig. 2). Magnetic susceptibility studies have proven particularly useful in characterizing the stratigraphic boundaries of soil–loess sequences in China (Liu, 1985; Kukla, 1987; Kukla and An, 1989). The susceptibility signal is greater in soils than in loess. Magnetic susceptibility of the Changwu and Weinan sections was measured on dry samples using a Bartington susceptibility meter. Samples for Weinan were taken at 10 cm intervals while those for Changwu were taken at 2.5 cm intervals for the S0–S5 sequence, at 5 cm intervals for the L6–L9 sequence, and at 10 cm intervals for the S9–L15 sequence. The susceptibility time series of the Xifeng section is from Kukla et al. (1990). The timescales for Changwu and Weinan are obtained by correlation with the Xifeng susceptibility curve (Fig. 2). The last is dated by a magnetic susceptibility model (Kukla and An, 1989). Although this model is based on some assumptions which are contentious in part (Heller et al., 1993; Verosub et al., 1993; Han et al., 1996), it remains a working model for obtaining an independent timescale until better methods are developed.

The paleosols and loess of the last 1.2 Ma in Weinan and Xifeng were studied by micromorphological methods (Table 1). Munsell colors (on soils in a humid state) were measured to evaluate the intensity of soil reddening. The content of primary carbonate and clay coatings, the abundance of Fe–Mn features, and the content of the fine fraction (< 10 μm) were estimated as a surface area percentage on thin sections under a microscope using a cross-lined micrometer. The free Fe_2O_3 (Fed), extracted by the citrate-bicarbonate-dithionite (CBD) method (Mehra and Jackson, 1960) and total Fe_2O_3 (Fet) extracted on acid-dissolved samples (McKeague, 1981), were analyzed on some Xifeng and Changwu area samples for characterizing the soil weathering intensity. The clay fraction (< 2 μm) of three samples from the Bt horizon of the S4, S5-1 and S5-3 soils in Weinan was analyzed by X-ray fluorescence method using a Philips PW-1400 unit for determining the SiO_2/Al_2O_3 molecular ratio.

3. Climatic extremes recorded in loess

3.1. Macro- and micro-morphology

In the Loess Plateau region, the Holocene soil (S0) is differentiated from the older soils by its dark color, weak rubification, and absence of clear calcitic horizons (Guo et al., 1991, 1993a,b, 1994; Liu et al., 1996), as is also the case for the studied sites. The paleosols in the Lishi Loess (from S1 to S15) are generally rubified and characterized by a B1-B2(or B2t)-BC-Ca-C horizon sequence. The lack of a clearly expressed A horizon is partly due to a slight truncation of the top part of some soils (e.g., S1 and S5-1 in Xifeng; Guo et al., 1991) and also due to the intensification of dust deposition during the late stage of soil formation while pedogenic processes were still operating (Guo et al., 1991). The calcitic horizons generally consist of hard nodules distributed in a relatively loose matrix (Guo and Fedoroff, 1990). The soil horizons with highest magnetic susceptibility (B2 or B2t) usually represent the most rubified, strongly decalcified, and contain high levels of clay coating. The Munsell color code and the major morphological features of the paleosols in Xifeng and Weinan are given in Table 1. The field morphology of the paleosols in Changwu is close to those in Xifeng, but they are slightly more developed, as is consistent with the magnetic susceptibility values (Fig. 2) and the Fed/Fet ratio (Fig. 3).

The S4, S5-1, S5-3 and S13 soils represent the most rubified soils (Table 1). They have a 5 YR hue in Xifeng compared to 10 YR to 7.5 YR for the other soils in the same section and the first two attain a 2.5 YR hue in Weinan. These soils are characterized by abundant reddish iron oxide/hydroxides particles (2–5 μm and finer) in the fine fraction, suggesting that the reddish color is closely associated with these iron particles.

The S4, S5-1 and S5-3 soils are totally decalcified in both sections and have the maximum amount of

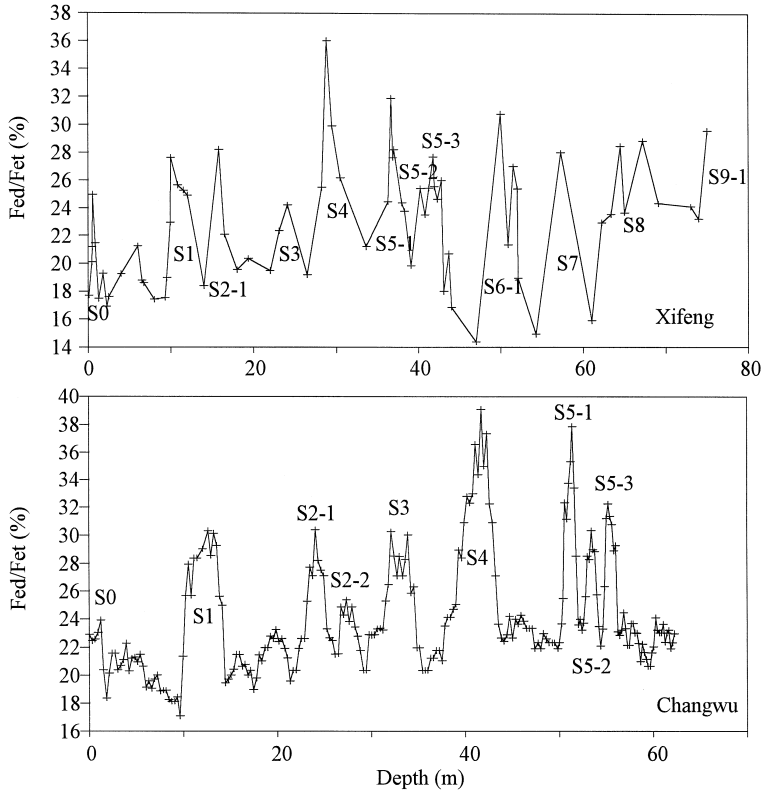

Fig. 3. Variations of the free Fe_2O_3 and total Fe_2O_3 ratio (Fed/Fet) in the Xifeng and Changwu loess sections. The sample resolution in Xifeng is irregular and that for Changwu is at 30 cm intervals from S0 to L4, at 20 cm intervals from S5 to L6.

textural features (clay coatings) (Table 1). Under microscope, the clay coatings are reddish brown, moderately laminated with strong birefringence. The more abundant fine fraction in these soils indicates stronger pedogenesis in comparison with the other soils. Although S13 is among the most rubefied of soils, non-clay coating soils were observed in Xifeng and the amount was much lower than for S4, S5-1 and S5-3 in Weinan.

In the field, the sandy loess units L9 and L15 are characterized by coarser texture, a paler color (10 YR 8/2-4) and greater friability, compared with the other loess units. The L9 unit consists of three sub-parts: the coarser upper and lower parts (corresponding to the marine $\delta^{18}O$ stages 22 and 24, respectively) and the finer middle part (to $\delta^{18}O$ stage 23) comparable to the other loess units, and is consistent with the variations in magnetic susceptibility (Fig. 2). The grain-size variations of several loess sections were measured (e.g., Liu and Ding, 1993; Ding et al., 1994; Vandenberghe et al., 1997), which showed that the loess units L9 and L15 represent the coarsest loess of the last 2.5 Ma.

The coarser texture of the sandy loess is expressed by a greater proportion of coarse silt (25–50 μm), up to 45–60% (from Weinan to Xifeng, by surface estimates), compared with about 30–40% for the other loess units. The sandy fraction is slightly more abundant (12–15%) than for the other loess units (8–10%). They are characterized by few channels and only traces of scarce biological activity. The detrital carbonate (about 15%) has relatively fresh morphology. The groundmass contains a large amount of sand-sized (60–300 μm), rounded to subrounded aggregates (pseudo-sands) consisting of silty mineral grains inbedded in the fine fraction. Some fragments of similar size, derived from soil materials and from soil surface crusts, are also ob-

served. This kind of microstructure has been described as 'pseudo-sand microstructure' (or 'pellet fabric') (Guo et al., 1993a, 1996a). It is interesting to note that the morphological features of these loess units are relatively similar for the studied sites, although the modern climate conditions in each location are quite different.

3.2. Weathering intensity of soils

The ratio of free Fe_2O_3 (Fed) and total Fe_2O_3 (Fet) contents is considered a measure of weathering intensity of soil horizons (e.g. Duchaufour, 1983). The variations of the Fed/Fet ratio from S0 to S9 of the Xifeng section and from S0 to L6 of the Changwu section (Fig. 3) are given to characterize the soil weathering intensity. It shows that the S4, S5-1 and S5-3 are among the most strongly weathered soils in the studied sequence. The distribution of Fed/Fet values in Changwu is coherent with the other pedological features, while those in Xifeng are less consistent (e.g., for S6). The discrepancy for Xifeng may be due to a much lower sample resolution than for Changwu. Since the average soil temperature in the Loess Plateau region are below 0°C from late autumn to early spring under the modern interglacial conditions (Institute of Soil Sciences, Academia Sinica, 1978), the weathering intensity of the soils mainly depends upon the summer temperature and precipitation. Consequently, higher weathering intensity for S4, S5-1 and S5-3 can be interpreted as an indication of more humid and warmer conditions, as is consistent with the interpretations based on morphological features.

3.3. Clay morphology and soil chemistry

The clay mineralogy and chemical properties of the Xifeng paleosols were analyzed (Guo, 1990, Guo et al., 1991) using X-ray diffraction. The clay mineralogy assemblage is dominated by illite, kaolinite, chlorites and smectites with more smectites in the S5-1 and S5-3 soils, as found by Liu (1985) for Luochuan. Another section near Xian, about 40 km in the southwest of Weinan, shows a similar mineralogical assemblage, but with a significantly greater amount of smectites and lower crystallinity of illites (Guo, 1990). These results indicate that the clay fraction is dominated by 2:1 type minerals, and the weathering is in a stage of *bisiallitisation* according to Pedro (1979).

In both Xifeng and Xian, all the soils are basic and the absorptive complex is saturated. The exchangeable cations are dominated by Ca^{2+} and Mg^{2+} (Guo, 1990; Guo et al., 1991). Analyses on the clay fraction ($< 2\ \mu m$) of the three samples from the Bt horizon of the Weinan soils show a SiO_2/Al_2O_3 molecular ratio of 3.42 for S4, 3.04 for S5-1 and 3.41 for S5-3.

3.4. Magnetic susceptibility

The magnetic susceptibility for Chinese loess-paleosol sequences is widely used as a climate proxy (e.g., Liu, 1985; Kukla and An, 1989; An et al., 1991a,b; Liu and Ding, 1993). Susceptibility values are higher in paleosols than in the overlying and underlying loess, and the causes remain contentious, and can be summarized as a *depositional* view, a *pedogenic* view, or a combination of both, as extensively reviewed by several authors (Heller et al., 1993; Hunts et al., 1995; Han et al., 1996).

The results in this study suggest that using magnetic susceptibility as climate proxy is partly valid for the sites studied. Several aspects seem to support the pedogenic point of view.

(1) The susceptibility values generally increase from northwest (Xifeng) to southeast (Weinan), and are consistent with the climatic pattern of the Loess Plateau region. The small differences between Xifeng and Changwu are consistent with the pedological features observed in the field.

(2) The well-developed S5-1 soil has the highest susceptibility values in Xifeng and Changwu.

(3) The susceptibility gradient of the studied sites is greater for paleosols and weak for most of the loess units. The sandy loess units L9 and L15 have the lowest values and are indeed comparable for the studied sites, as is coherent with the morphological features.

Several points, however, need to be noted for a temporal examination.

(1) For all of the three localities, the S4, S5-1 and S5-3 soils represent the most developed soils (Table 1 and Fig. 3), while the susceptibility values for S4

and S5-3 are not higher than for the other soil units (Fig. 2).

(2) In Weinan, the paleosol S1 is much less developed than S4, S5-1 and S5-3, while its susceptibility values represent the highest of the whole section (Fig. 2).

(3) The paleosol S13 is significantly more developed than, for example, S2 and S3 (Table 1 and Fig. 3), while its susceptibility values are much lower than these soils (Fig. 2).

(4) A most puzzling aspect, difficult to explain from a simple *pedogenic* point of view, arises from the three sub-units of the S5 unit: the intensity of pedogenesis shows, in order, S5-1 (highest), S5-3 to S5-2 (weakest), while the susceptibility values show, in order, S5-1 (highest), S5-2 to S5-3 (lowest). The susceptibility values for the major soil units older than S5-1 are much lower than for the younger interglacial soils (S0 to S5-1), even lower than for some weakly developed interstadial soils in the loess units L1, L2 and L3.

Our results, therefore, provide a complex picture for the climatic significance of magnetic susceptibility in paleosols. The susceptibility value is not always consistent with other parameters and the mechanism is not clear, and thus needs additional work. Several processes may have to be comprehensively considered in future studies: (1) transformation/neoformation of magnetic minerals in soils following the types and intensity of pedogenesis; (2) changes in aeolian dust composition for different interglacial periods associated with possible changes in wind patterns and source areas; (3) particle sorting of aeolian dust during transportation that may lead to a spatial sorting of dust composition; and (4) local sources of aeolian dust.

3.5. Climate interpretations

The above data show that the S4, S5-1, and S5-3 soils represent the most developed soils with S5-1 being the most intense, as indicated by strong rubification, lack of primary carbonate, higher contents in clay coatings in Fe–Mn features and in the fine fraction (Table 1), and higher Fed/Fet ratios.

It is commonly considered that soil reddening processes are typical of warm and relatively humid environments (e.g. subtropical to tropical) and that the most favorable conditions occur when the climates show strong seasonal contrast (Bresson, 1976; Schwertmann et al., 1982; Duchaufour, 1983). This is consistent with the seasonality of the monsoonal climate prevailing the Loess Plateau region. It has been demonstrated that Holocene rubefication is rather weak and thus is not a typical pedogenic process in the Loess Plateau region (Guo et al., 1993a, 1994; Liu et al., 1996). The strong rubefication of the S4, S5-1 and S5-3 soils can therefore be considered as an indication of much warmer conditions than for the present-day average. The increasing intensity of rubification from northwest (Xifeng) to southeast (Weinan) is consistent with the intensity pattern of pedogenesis observed in the Loess Plateau region.

The relative abundance of clay coatings can be regarded, to some extent, as an indication of the quantity of percolating water (Duchaufour, 1983) which is closely related to the annual rainfall. For the soils studied in this analysis, their clay content is generally consistent with the amount of Fe–Mn as seen in S5-1 (Table 1). The absence of clay coatings and Fe–Mn features in Xifeng and the lesser amount in Weinan for the S13 soil suggest a drier soil water regime than when S4, S5-1 and S5-3 were formed. The higher content in clay coatings and especially Fe–Mn features in the S4, S5-1 and S5-3 soils, compared with the others, indicates greater soil humidity. The amount of clay coatings and Fe–Mn features, the soil chemical properties, as well as the presence of a calcitic horizon for all the soils, however, preclude the possibility of prolonged soil humidity. The clay coatings are reddish brown, microlaminated with strong birefringence. These illuvial features are commonly interpreted as evidence of broadleaf forest soils (Fedoroff and Goldberg, 1982; Avery, 1985), and the strong reddish hue of the clay coating is typical of subtropical to tropical environments (Fedoroff and Rodriguez, 1978; Cremaschi, 1987). The S4, S5-1 and S5-3 soils, therefore, provide evidence for a relatively large increase in summer soil temperature and a moderate increase in soil humidity, probably due to the strong evapotranspiration related to higher soil temperatures. We interpret these soils as forest–steppe soils with accentuated forest cover during the climatic optimum. In Xifeng and Changwu, they can be tentatively classified as

transitional Luvic Kastanozems (with chromic characters) to Chromic Luvisols according to the FAO soil classification system (Fao-Unesco, 1974). This corresponds approximately to red-brown soils of some genetic classification systems (Zhu, 1985). Those at Weinan may be classified as Chromic Luvisols. It is difficult to find a modern soil type in China exactly analogous to the soils studied, but the soil-forming processes are comparable to those in the subhumid region in mid-southern China, ascribed as argillic eutrophic brown-red soils (STCRG and CRGCSTC, 1991). They are also somewhat similar to the red-brown soils in modern subhumid subtropical zones in Africa and the Mediterranean region (Duchaufour, 1976; Zhu, 1985). In comparison with the modern conditions of the sites studied, we estimate tentatively for the S5-1 soil, an approximate increase of at least 4–6°C for the annual mean temperature and an increase of 200–300 mm for the annual rainfall. For the southern Loess Plateau (Weinan), these imply a temperature regime close to that in the southern Yangtz River basin at present and a precipitation regime close to that of the Huaihe River basin for the present day. In comparison with the S5-1 soil, the conditions for S4 and S5-3 should be slightly drier.

Recently, several climofunctions have been developed based on magnetic susceptibility for quantitative estimates of paleoclimates and were applied on the loess-paleosol sequences of the last climatic cycle (Lu et al., 1994; Maher and Thompson, 1995; Han et al., 1996). These functions were developed using a large number of surface samples taken from the loess-like silt-covered regions in China. Application of this method to some older soils can only be considered partly valid because of the susceptibility anomalies discussed above. However, an attempt on the S5-1 soil may be more indicative, as its high susceptibility values seem to be in agreement with the other features (Table 1 and Fig. 3). Tentative estimates for Xifeng and Changwu yield a mean annual temperature of about 14°C, and a mean annual precipitation of about 800 mm (Fig. 4), which seems to be consistent with the above estimates based on soil properties. Since the high susceptibility values in Weinan soils largely exceed the valid range of this climofunction, the results should be considered questionable.

The paleosol evidence from S4, S5-1 and S5-3 represent the three periods of greatest warmth of the last 1.2 Ma with S5-1 formed during the period of greatest warmth and humidity. As the climate of the

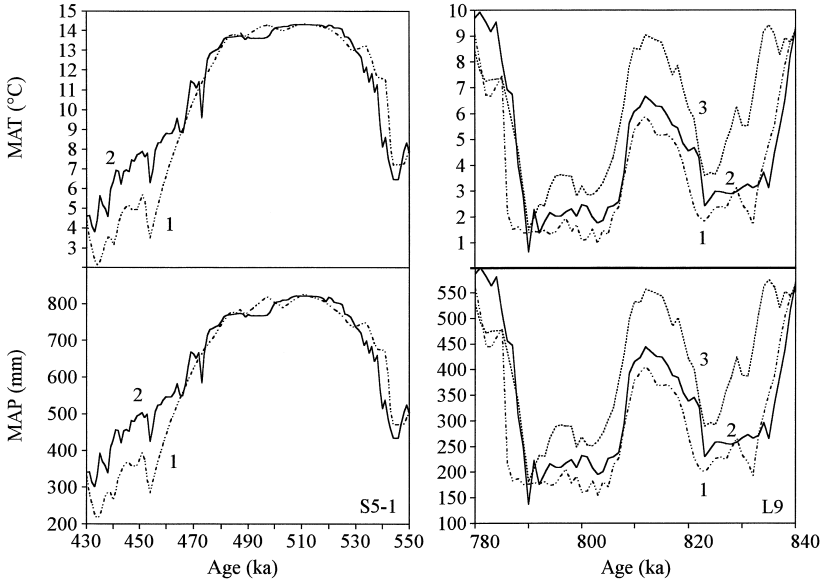

Fig. 4. Tentative quantitative estimates of paleoclimates for S5-1 and L9 based on the climofunction of Lu et al. (1994) and Han et al. (1996). 1. Xifeng; 2. Changwu; 3. Weinan.

Loess Plateau region is controlled by the monsoon (Zhang and Lin, 1987), episodes of great warmth can be interpreted as evidence of particularly strong summer monsoons. The similarity of the soils between Xifeng and Changwu (Fig. 2) indicates that the climate gradient between the two sites was rather weak. However, the clay coatings, Fe–Mn features and the fine fractions in the Weinan soils are much more abundant than for the two other sites, suggesting that the increase in the annual rainfall was particularly accentuated for the southern-most part of the Loess Plateau. This may imply that the monsoon rain belt (the so-called 'Meiyu belt') affects the southern-most part of the Plateau for a relatively long period each year. Under the modern conditions, this belt usually reaches and remains across the Yangtz-Huaihe River basins (between 26–34° N in eastern China) from early June to early July of each year, resulting in a long and continuous rainy season for the region.

It is commonly considered that the desertic lands in northwestern China and central Asia are the source areas of loess, and the dust is transported by northwesterly winter monsoon winds (An et al., 1991a). Consequently, the grain-size variations of loess depend on the strength of the winter monsoon (Liu and Ding, 1993; Vandenberghe et al., 1997) and also on the distance from the source areas. The sandy loess L9 and L15 can therefore be interpreted as evidence of particularly strengthened winter monsoon winds and a southward extension of the desertic lands. The weak biological activity in these loess units indicates a quite sparse vegetation cover, unable to provide enough organic matter for soil fauna. These two loess units have a *pseudo-sand* microstructure (or pellet fabric). According to Pye and Tsoar (1987), particles larger than 100 μm are weakly transported over long distances as suspended dust, and most is deposited within 30 km of their source. These pseudo-sands were evidently derived from local loess material, rather than typical desert aeolian dust particles. Since reworking by water is not observed in these loess profiles, the pseudo-sands must have been produced by aeolian erosion of previously deposited loess and soils, and transported by saltation, as is indicated by their rounded to subrounded edges. This interpretation is also supported by the fragments of soil and surface crust, which is indicative of soils with sparse vegetation cover (Courty and Fedoroff, 1985). The pseudo-sand microstructure and the fragments of soil material therefore imply an aeolian erosion of the land surface with sparse vegetation cover. The relatively fresh morphology of detrital carbonate in the groundmass indicates a low annual rainfall. The L9 and L15 loesses provide evidence of a semi-desertic landscape, with strengthened aeolian deposition. A tentative application of the climo-function of Lu et al. (1994) yields a mean annual temperature of about 1.5–3°C and a mean annual precipitation of about 150–250 mm (Fig. 4). These values are consistent with the pedological interpretations and imply a landscape comparable to that of the present-day northeast Inner Mongolian region. This now lies beyond the modern summer monsoon influence. The similarity in morphology and magnetic susceptibility values of the three studied sites (Fig. 2) indicates a very weak climate gradient in the Loess Plateau region. During the deposition of these loess units, the summer monsoon rarely penetrated into the Loess Plateau region.

4. Correlation of the climate extremes with marine δ^{13}C records

The variations in global ice volume, as indicated by the marine δ^{18}O record, and orbitally induced insolation changes, have been previously invoked to explain the long-term changes in east Asian monsoon climate (An et al., 1991a; Liu and Ding, 1993; Guo et al., 1994; Liu et al., 1995; Ding et al., 1995). However, the great warmth reflected by S4, S5-1 and S5-3 soils, and the severe dry-cold periods evidenced by the L9 and L15 loess cannot be convincingly explained by either global ice-volume variations or insolation changes (Fig. 2), as the corresponding ice volumes were not less than for the other interglacial stages, and the insolation values for the northern hemisphere were not higher (Fig. 2), except for the L15, which seems to correspond to lower-than-average ETP values. Examination of several marine records shows that δ^{18}O values were approximately similar during stages 15, 13, 11, 9, 5 and 1 (e.g., Imbrie et al., 1984; for a SPECMAP composite δ^{18}O record; the composite δ^{18}O record proposed by Williams et al., 1988; DSDP-552 and ODP 677

$\delta^{18}O$ records from Shackleton and Hall, 1984, 1989), except for the North Atlantic Site 607 (Ruddiman et al., 1989) where, as Oppo et al. (1990) stated, only one data point from stage 11 is lower than the minima of marine isotope stages 9, 5 and 1 (Fig. 2). Thus, the available data suggest that, in most records, $\delta^{18}O$ values were not lower during stages 15, 13 and 11 than during other interglaciations. These imply that other important factors must have operated during the formation of S4, S5-1 and S5-3 soils.

Ocean circulation is one of the most important forcing factors of the Earth-climate system. The North Atlantic Deep Water (NADW) played a vital role in modulating the world ocean circulation pattern (Raymon et al., 1990). Variations of the NADW strength may be an important factor controlling glacial–interglacial changes in atmospheric CO_2 (Boyle, 1988; Broecker and Peng, 1989). The changes in NADW may have been responsible for the Younger Dryas cooling event (Jansen and Veum, 1990) and for the high-frequency changes in the last glacial period (Kelgwin et al., 1994) of which the signals have been identified in a number of terrestrial records in China (Porter and An, 1995; Guo et al., 1996c). We might therefore expect that variations of the NADW production would have significant consequences on the monsoon climate in China.

$\delta^{13}C$ is a useful tracer of paleoceanographic changes in deep water circulation (Curry et al., 1988; Raymon et al., 1990). The benthic $\delta^{13}C$ gradient between the Atlantic and Pacific oceans has been used to evaluate the strength of the NADW production of the last 2.5 Ma (Raymon et al., 1990). The NADW, which is formed with an initial high $\delta^{13}C$ value becomes gradually lower in $\delta^{13}C$ as it flows southward to the Pacific Ocean and through mixing with Southern Ocean water (SOW) and aging (Raymon et al., 1990). Another important factor for $\delta^{13}C$ values is the organic carbon sequestered on continents. Since the last glaciation, an increase in continental biomass has resulted in a estimated 3.2‰ rise in the average carbon isotopic composition of the oceans (Duplessy et al., 1988). Because this change is imbedded within all oceanic $\delta^{13}C$ records equally, it does not affect $\delta^{13}C$ gradients within the ocean (Raymon et al., 1990). Therefore, the ocean $\delta^{13}C$ values mainly reflect both NADW production and continental biomass, while the $\delta^{13}C$ gradient between the Atlantic and the Pacific is mainly an indication of the strength of NADW production (Curry et al., 1988; Raymon et al., 1990).

In Fig. 5, the studied soil–loess sequence, represented by the magnetic susceptibility time-series, is compared with the fluctuations of benthic $\delta^{13}C$ values from the North Atlantic DSDP Site 552 (Shackleton and Hall, 1984) and DSDP Site 607 (Ruddiman et al., 1989) and the equatorial Pacific ODP Site 677 (Shackleton and Hall, 1989). The three sites are thought to be well located for tracing the strength of the NADW production (Raymon et al., 1990).

The strongly developed S4, S5-1, and S5-3 soils match well with the higher $\delta^{13}C$ values in both Atlantic and Pacific oceans (Fig. 5). The high $\delta^{13}C$ values during these stages are more clearly expressed at the Pacific site RC13-110 (Mix et al., 1991), located at a similar depth to the ODP Site 677. These agreements can be explained by strong NADW production or/and land biomass increase. In both cases, these imply that the periods of great warmth recorded in loess of China are not local phenomena, but represent global changes in the land–sea configuration pattern as they affect the carbon reservoirs. This was different during marine stages 11, 13 and 15 to interglacials, so that the world ocean $\delta^{13}C$ values were affected. The correlation also indicates that the strong development of these soils is not solely a function of longer soil-forming duration but of climate conditions accompanied by a strengthened summer monsoon.

The $\delta^{13}C$ gradient between the Atlantic and Pacific can be regarded as an indication of the NADW strength. Closer $\delta^{13}C$ values between DSDP Sites 552 and 607, and larger differences between the Atlantic and Pacific, imply increased NADW strength, as does the inverse (Raymon et al., 1990). Fig. 5 shows that during the formation of S4 and S5-3 soils, the Atlantic–Pacific gradients are greater than any other interglacial period of the last 1.2 Ma, suggesting stronger NADW production. Consequently, the high $\delta^{13}C$ values in both the Atlantic and Pacific oceans cannot be solely explained by land biomass increase, but are related to strong NADW production. The case of the S4 soil is consistent with the conclusion of Oppo et al. (1990) that the NADW was particularly strong during $\delta^{18}O$

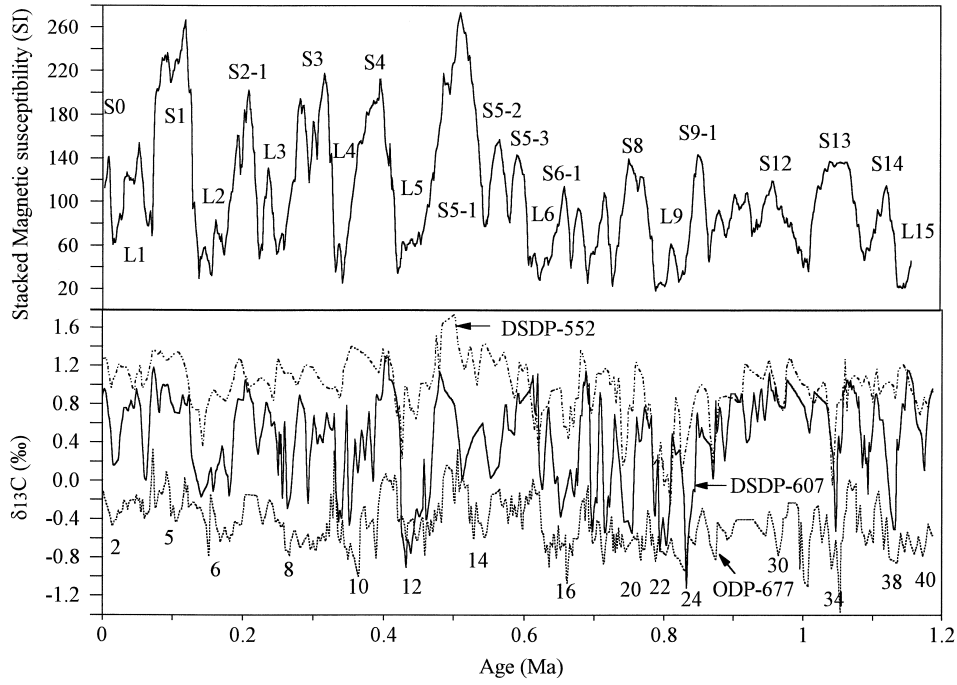

Fig. 5. Correlation of the loess–paleosol sequences as reflected by the stacked magnetic susceptibility curve with marine $\delta^{13}C$ records. The stacked susceptibility curve is obtained by averaging the Xifeng, Changwu and Weinan susceptibility after equally spacing the data in time. The $\delta^{13}C$ timeseries are from Raymon et al. (1990), which are derived from the Atlantic DSDP Site 552A (Shackleton and Hall, 1984), the Atlantic DSDP Site 607 (Ruddiman et al., 1989) and the Pacific ODP Site 677 (Shackleton and Hall, 1989). The oxygen isotope stages are labeled.

stage 11 and that the North Atlantic polar front and southern Indian Ocean subtropical convergence zone were located further poleward during stage 11 than in other more recent stages.

During the formation of the S5-1 soil, $\delta^{13}C$ values in both the Atlantic and Pacific were considerably higher than other interglacial periods while the gradients remain moderate. This phenomenon may be explained by two alternative possibilities.

(1) During formation of the S5-1 soils, the NADW production was moderate, comparable to the interglacial periods (other than stages 11 and 15), but other factors had considerably modulated the climate conditions in Asia, which induced a significant increase in land biomass and, thus, enhanced the ocean $\delta^{13}C$ values. These factors must have been of large scale or of global extent but not directly related to either ice-sheet forcing or insolation changes. If the atmospheric CO_2 level is closely related to the strength of NADW production, as suggested by a number of authors (Boyle, 1988; Broecker and Peng, 1989), these factors are also unlikely to be related to the greenhouse effect of the raised atmospheric CO_2 level during interglacials.

(2) The great warmth reflected by the S5-1 soil was still related to a strengthened NADW production, but the $\delta^{13}C$ values of one (or more) of the sites for stage 13 were affected by factors other than land biomass and NADW strength, so that they underestimate the NADW strength.

The second possibility is supported by the comparison of $\delta^{13}C$ values between RC13-229 (Southern Ocean) and Pacific V19-30 and ODP 677 sites (see Oppo et al., 1990): during stages 11 and 13, the $\delta^{13}C$ differences between the Pacific and Southern oceans were significantly greater than during other interglacial stages, indicating greater flux of NADW to the Southern Oceans (Oppo et al., 1990).

According to the commonly accepted land–sea correlation (Fig. 2), the sandy loess L9 and L15

correlate to marine $\delta^{18}O$ stages 22, 23, 24 and 38, respectively. During stages 22, 24 and 38, the Atlantic/Pacific $\delta^{13}C$ values converge (Fig. 5), indicating very weak or suppressed NADW production, as stated by Raymon et al. (1990). A similar reduction of NADW has been reported by Raymon et al. (1990) for marine $\delta^{18}O$ stage 12, corresponding to the L5 loess in China. In fact, this loess is also characterized by a pseudo-sand microstructure and weak biological activity (Guo et al., 1993a), and a coarser-than-average grain size (Vandenberghe et al., 1997).

Our results, therefore, suggest that the two kinds of climate extremes recorded in the loess-paleosol sequences of the last 1.2 Ma in China reflect large regional or global events, which match variations in the strength of the North Atlantic Deep Water production. The periods of great warmth, evidenced by the S4, S5-1 and S5-3 soils, are linked in time with particularly strengthened NADW production while the severest glacial periods, evidenced by L9 and L15, match the periods with weak or suppressed NADW production. These indicate that both the summer and winter monsoons in the Loess Plateau region are linked with the NADW production.

Climatic signals in relation with the North Atlantic Heinrich events have been reported based on the grain-size variations of loess (Porter and An, 1995), and on the paleo-weathering time-series (Guo et al., 1996b). As Heinrich events are thought to be linked with the changes in the NADW strength (Kelgwin et al., 1994), the results here are highly supportive of our previous deduction that the North Atlantic Heinrich signals were not only linked with the Asian winter monsoon, as indicated by Porter and An (1995), but also with the summer monsoon circulation (Guo et al., 1996b).

The mechanism linking the NADW strength and that of the monsoon climate of the Loess Plateau remains unclear and needs additional work. Two possibilities may be invoked to explain this link. Firstly, the NADW strength may be an important forcing factor controlling the strength of the East Asian summer and winter monsoons, and played a vital role in modulating the world ocean circulation pattern, and thus the global heat distribution (Raymon et al., 1990). This link might also be attributable to the greenhouse effect of the atmospheric CO_2 which is thought to be strongly controlled by the NADW production (Boyle, 1988; Broecker and Peng, 1989). The important increase in soil temperature against a moderate increase in soil humidity as indicated by the S4, S5-1 and S5-3 seems to support this hypothesis. An alternative possibility is that some common factors controlled both Asian monsoon strength and NADW production duting the formation of these soil and loess units.

5. Conclusions

Our results have therefore demonstrated that the loess-paleosol sequences have recorded two kinds of climate extremes: periods of great warmth evidenced by the S4, S5-1 and S5-3 soil units, and very sever glacial periods reflected by the loess units L9 and L15. They cannot be convincingly explained by either ice-volume forcing and insolation changes, the two main factors invoked in earlier studies for explaining the long-term variations of paleoclimates in the Loess Plateau region (e.g. An et al., 1991b; Liu and Ding, 1993; Guo et al., 1994; Ding et al., 1995; Liu et al., 1995).

The paleopedological, geochemical and magnetic susceptibility data suggest that S4, S5-1 and S5-3 were formed under sub-tropical semi-humid environments. Tentative estimates for the S5-1 soil yield a mean annual temperature (MAT) of about 4–6°C higher and a mean annual precipitation (MAP) of 200–300 mm higher than for the present-day average. During the formation of these soils, the increase in the annual rainfall was particularly accentuated for the southern-most part of the Loess Plateau, indicating that the plateau was strongly influenced by the summer monsoon. The monsoon front might stabilize over the southern-most part of the plateau for a relatively long period each year, as is the case for the Yangtz–Huaihe basin in southern China at the present-day. The sandy loess units L9 and L15 were deposited under semi-desertic environments with an MAP and MAT of about 1.5–3°C and 150–250 mm, respectively. The climatic gradient was rather weak, suggesting that the Loess Plateau climate was strongly controlled by the dry-cold winter monsoon and that the summer monsoon front could rarely penetrate into the region.

The synchronous changes in benthic $\delta^{13}C$ values of the world ocean indicate that the climate extremes have large regional, and possibly even global, significance. This also implies that the strong development of Loess Plateau soils is not solely a function of time but of climate conditions associated with strengthened summer monsoon.

Correlation with the $\delta^{13}C$ pattern of the world ocean indicates that the two kinds of climate extremes match the episodes with greatest/smallest ocean $\delta^{13}C$ gradients, respectively, implying their relationship with the strength of the deep-water formation in the North Atlantic. These results suggest that both summer and winter monsoon circulation patterns prevailing over the Loess Plateau region in China are linked with the NADW strength on timescales of 10^4 years.

Acknowledgements

This work was supported by the National Natural Science Foundation of China and the Chinese Academy of Sciences. The authors thank Dr. Z. Gu for field collabaration in Weinan, and for part of the Weinan magnetic susceptibility data. Z. Guo is grateful to Dr. M.A. Courty, Professors M. Fontugne and J. Guiot for valuable discussions and suggestions. Sincere thanks are extended to Prof. J. Dodson and two anonymous reviewers for a critical review and language improvement of the manuscript.

References

An, Z.S., Wei, L.Y., 1980. The fifth paleosol in the Lishi Loess and its paleoclimatic significance. Acta Pedologica Sinica 1, 1–12, (in Chinese with English abstract).

An, Z.S., Liu, T.S., Lu, Y.C., Porter, S.C., Kukla, G., Wu, X.H., Hua, Y.M., 1991a. The long-term paleomonsoon variation recorded by the loess-paleosol sequence in central China. Quat. Int. 7–8, 91–95.

An, Z.S., Kukla, G., Porter, S.C., Xiao, J.L., 1991b. Magnetic susceptibility evidence of monsoon variation on the loess plateau of central China during the last 130,000 years. Quat. Res. 36, 29–36.

Avery, B.W., 1985. Argillic horizons and their significance in England and Wales. In: Boardman, J. (Ed.), Soils and Quaternary Landscape Evolution. Wiley, London, pp. 68–86.

Berger, A., Loutre, M.F., 1991. Insolation values for the climate of the last 10 million years. Quat. Sci. Rev. 10, 297–317.

Billard, A., 1993. Is a middle Pleistocene climatic optimum recorded in the loess-paleosol sequences of Euroasia?. Quat. Int. 17, 87–94.

Boyle, E.A., 1988. The role of vertical chemical fractionation in controlling late Quaternary atmospheric carbon dioxide. J. Geophys. Res. 93, 15701–15714.

Bresson, L.M., 1976. Rubéfaction récente des sols sous climat tempéré humide: séquence évolutive sur fluvio-glaciaire calcaire dans le Jura méridional (Etude de microscopie intégrée). Science du Sol 1, 3–22.

Broecker, W.S., Peng, T.H., 1989. The cause of the glacial to interglacial atmospheric CO_2 change: a polar alkalinity hypothesis. Global Geochem. Cycles 3, 215–240.

Bronger, A., Heinkele, T.H., 1989. Micromorphology and genesis of paleosols in the Luochuan loess section, China: pedostratigraphic and environmental implications. Geoderma 45, 123–143.

Clemens, S., Prell, W., Murray, D., Shimmield, G., Weedon, G., 1991. Forcing mechanisms of the Indian Ocean monsoon. Nature 353, 720–725.

Courty, M.A., Fedoroff, N., 1985. Micromorphology of recent and buried soils in a semi-arid region of Northwest India. Geoderma 35, 287–332.

Cremaschi, M., 1987. Paleosols and vetusols in the central Po Plain (Northern Italy), a study in Quaternary geology and soil development. Edizioni Unicopli, Milano, 306 pp.

Curry, W.B., Duplessy, J.C., Labeyrie, L.D., Shackleton, N.J., 1988. Changes in the distribution of $\delta^{13}C$ of deep water CO_2 between the last glaciation and the Holocene. Paleoceanography 3, 317–341.

Ding, Z.L., Yu, Z.W., Rutter, N.W., Liu, T.S., 1994. Towards an orbital time scale for Chinese loess deposits. Quat. Sci. Rev. 13, 39–70.

Ding, Z.L., Liu, T.S., Rutter, N., Yu, Z.W., Guo, Z.T., Zhu, R.X., 1995. Ice-volume forcing of east Asian winter monsoon variations in the past 800,000 years. Quat. Res. 44, 149–159.

Duchaufour, Ph., 1976. Atlas écologique des sols du monde. Masson. Paris–New York–Barcelone–Milan, 178 pp.

Duchaufour, Ph., 1983. Pédologie, Tome 1: Pédogenèse et Classification. Masson, Paris-New York-Barcelone–Milan, 477 pp.

Duplessy, J.C., Shackleton, N.J., Fairbanks, R.G., Labeyrie, L., Oppo, D., Kallel, N., 1988. Deep water source variations during the last climatic cycle and their impact on the global deep-water circulation. Paleoceanography 3, 343–360.

Fao-Unesco, 1974. Soil Map of the World, Vol. 1. Legend, Paris.

Fedoroff, N., Goldberg, P., 1982. Comparative micromorphology of two late Pleistocene paleosols (in the Paris Basin). Catena 9, 227–251.

Fedoroff, N., Rodriguez, A., 1978. Micromorphologie des sols rouges de Tenerife et de La Palma (Iles Canaries), Comparaison avec les sols rouges méditerranéens. In: Delgado, M. (Ed.), Micromorfologia de Suelos. Granada, Espana, pp. 887–928.

Guo, Z.T., 1990. Succession des paléosols et des loess du centre-ouest de la Chine: approche micromorphologique. Thesis of Univ. Paris VI, France, 226 pp.

Guo, Z.T., Fedoroff, N., 1990. Genesis of calcium carbonate in loess and in paleosols in central China. Dev. Soil Sci. 19, 355–359.

Guo, Z.T., Fedoroff, N., An, Z.S., 1991. Genetic types of the Holocene soil and the Pleistocene paleosols in the Xifeng loess section in central China. In: Liu, T.S. (Ed.), Loess, Environment and Global Change. Science Press, Beijing, pp. 93–111.

Guo, Z.T., Fedoroff, N., Liu, T.S., 1993a. Paleosols as evidence of difference of climates between the Holocene and the Last Interglacial. Quat. Sci. 1, 41–55, (in Chinese with English abstract).

Guo, Z.T., Liu, T.S., Fedoroff, N., An, Z.S., 1993b. Shift of the monsoon intensity on the Loess Plateau at ca. 0.85 Ma BP. Chin. Sci. Bull. 38, 586–591.

Guo, Z.T., Liu, T.S., An, Z.S., 1994. Paleosols of the last 0.15 Ma in the Weinan loess section and their paleoclimatic significance. Quat. Sci. 3, 256–269, (in Chinese with English abstract).

Guo, Z.T., Ding, Z.L., Liu, T.S., 1996a. Pedosedimentary events in loess of China and Quaternary climatic cycles. Chin. Sci. Bull. 41, 1189–1193.

Guo, Z.T., Fedoroff, N., Liu, T.S., 1996b. Micromorphology of the loess-paleosol sequence of the last 130 ka in China and paleoclimatic events. Sci. China 39, 468–477, (Series D).

Guo, Z.T., Liu, T.S., Guiot, J., Wu, N.Q., Lu, H.Y., Han, J.M., Liu, J.Q., Gu, Z.Y., 1996c. High frequency pulses of east Asian monsoon climate in the last two glaciations: link with the North Atlantic. Climate Dynamics 12, 701–709.

Han, J.M., Lu, H.Y., Wu, N.Q., Guo, Z.T., 1996. The magnetic susceptibility of modern soils in China and its use for paleoclimatic reconstruction. Stud. Geophys. Geodaetica 40, 262–275.

Heller, F., Shen, C.D., Beer, J., Liu, X.M., Liu, T.S., Bronger, A., Suter, M., Bonani, G., 1993. Quantitative estimates of pedogenic ferromagnetic mineral formation in Chinese loess and palaeoclimatic implications. Earth Planet. Sci. Lett. 114, 385–390.

Hovan, S.A., Rea, D.K., Pisias, N.G., Shackleton, N.J., 1989. A direct link between the China loess and marine $\delta^{18}O$ records: aeolian flux to the north Pacific. Nature 340, 296–298.

Hunts, C.P., Banerjee, S.K., Han, J.M., Solheid, P.A., Oches, E., Sun, W.W., Liu, T.S., 1995. Rock–magnetic proxies of climate change in the loess-paleosol sequences of the western Loess Plateau of China. Geophys. J. Int. 123, 232–244.

Imbrie, J., Hays, J.D., Martinson, D., McIntyre, A., Mix, A.C., Morley, J.J., Pisias, N.G., Prell, W.L., Shackleton, N.J., 1984. The orbital theory of Pleistocene climate: support from a revised chronology of marine delta ^{18}O record. In: Berger, A., Imbrie, J., Hays, J., Kukla, G., Saltzman, B. (Eds.), Milankovitch and Climate, Part 1. Reidel, Dordrecht, Netherlands, pp. 265–305.

Institute of Soil Sciences, Academia Sinica, 1978. Soils in China. Science Press, Beijing (in Chinese).

Jansen, E., Veum, T., 1990. Evidence of two-step deglaciation and its impact on North Atlantic deep-water circulation. Nature 343, 612–616.

Kelgwin, L.D., Curry, W.B., Lehman, S.J., Johnsen, S., 1994. The role of the deep ocean in North Atlantic climate change between 70 and 130 kyr ago. Nature 371, 323–326.

Kukla, G., 1987. Loess stratigraphy in central China. Quat. Sci. Rev. 6, 191–219.

Kukla, G.J., An, Z.S., 1989. Loess stratigraphy in central China. Palaeogeography, Palaeoclimatology, Palaeoecology 72, 203–225.

Kukla, G., An, Z.S., Melice, J.L., Gavin, J., Xiao, J.L., 1990. Magnetic susceptibility record of Chinese loess. Trans. R. Soc. Edinburgh: Earth Sci. 81, 263–288.

Liu, T.S., 1985. Loess and the Environment. China Ocean Press, Beijing, 251 pp.

Liu, T.S., Yuan, B.Y., 1987. Paleoclimatic cycles in northern China. In: Liu, T.S. (Ed.), Aspects of Loess Research. China Ocean Press, Beijing, pp. 1–26.

Liu, T.S., Ding, Z.L., 1993. Stepwise coupling of monsoon circulation to global ice volume variations during the late Cenozoic. Global Planetary Change 7, 119–130.

Liu, X.M., Liu, T.S., Xu, T.C., Liu, C., Chen, M.Y., 1987. A preliminary study on magnetostratigraphy of a loess profile in Xifeng area, Gansu province. In: Liu, T.S. (Ed.), Aspects of Loess Research. China Ocean Press, pp. 164–174.

Lu, H.Y., Han, J.M., Wu, N.Q., Guo, Z.T., 1994. Magnetic susceptibility of the modern soils in China and paleoclimatic significance. Sci. China 24, 1290–1297, (Series-B) (in Chinese).

Liu, T.S., Guo, Z.T., Liu, J.Q., Han, J.M., Ding, Z.L., Gu, Z.Y., Wu, N.Q., 1995. Variations of eastern Asian monsoon over the last 140,000 years. Bull. Soc. Geol. Fr. 166, 221–229.

Liu, T.S., Guo, Z.T., Wu, N.Q., Lu, H.Y., 1996. Prehistoric vegetation on the Loess Plateau: steppe or forest?. J. Southeast Asian Earth Sci. 13, 341–346.

Maher, B.A., Thompson, R., 1995. Paleorainfall reconstructions from pedogenic magnetic susceptibility variations in the Chinese loess and paleosols. Quat. Res. 44, 383–391.

McKeague, J.A., 1981. Manual on soil sampling and methods of analysis. Can. Soc. Soil Sci., 212 pp.

Mehra, O., Jackson, M.L., 1960. Iron oxide removal from soil and clay by a dithionite–citrate system buffered with sodium bicarbonate. Clay and Clay Minerals 7, 317–327.

Mix, A.C., Pisias, N.G., Zahn, W., Rugh, C., Lopez, C., Nelson, K., 1991. Carbon 13 in Pacific deep and intermediate waters, 0–370 ka: implications for ocean circulation and Pleistocene CO_2. Paleoceanography 6, 205–226.

Oppo, D.W., Fairbanks, R.G., Gordon, A.L., 1990. Late Plieistocene southern ocean $\delta^{13}C$ variability. Paleoceanography 5, 43–54.

Pedro, G., 1979. Les conditions de formation des constituants secondaires. In: Bonneau, M., Souchier, B. (Eds.), Pédologie 2: Constituants et Propriétés du Sol. Masson, Paris–New York–Barcelone–Milan, pp. 58–72.

Porter, S.C., An, Z.S., 1995. Correlation between climate events in the North Atlantic and China during the last glaciation. Nature 375, 305–308.

Pye, K., Tsoar, H., 1987. The mechanics and geological implications of dust transport and deposition in deserts with particular reference to loess formation and dune sand disgenesis in the

northern Negev, Israel. Geological Soc. Special Publication 35, 139–156.

Raymon, M.E., Ruddiman, W.F., Shackleton, N.J., Oppo, D.W., 1990. Evolution of Atlantic–Pacific $\delta^{13}C$ gradients over the last 2.5 My. Earth Planet. Sci. Lett. 97, 353–368.

Ruddiman, W.F., Kutzbach, J.E., 1989. Forcing of late Cenozoic northern hemisphere climate by plateau uplift in southern Asia and the American West. J. Geophys. Res. 94, 18409–18427.

Ruddiman, W.F., Raymon, M.E., Martinson, D.G., Clement, B.M., Backman, J., 1989. Pleistocene evolution: northern hemisphere ice sheets and North Atlantic Ocean. Paleoceanography 4, 353–412.

Rutter, N., Ding, Z.L., Liu, T.S., 1991. Comparison of isotope stage 1–61 with the Baoji-type pedostratigraphic section of north–central China. Can. J. Earth Sci. 28, 985–990.

Schwertmann, U., Murad, E., Schulze, D.G., 1982. Is there Holocene reddening (hematite formation) in soils of axeric temperate areas?. Geoderma 27, 209–223.

Shackleton, N.J., Hall, M.A., 1984. Oxygen and carbon isotope stratigraphy of deep-sea drilling project Hole 552A: Plio–Pleistocene glacial history. Initial Reports of the Deep-Sea Drilling Project 81, pp. 599–609.

Shackleton, N.J., Hall, M.A., 1989. Stable isotope history of the Pleistocene at ODP 677. Proceedings of the Ocean Drilling Program, Scientific Results 111, 295–316.

STCRG (Soil Taxonomic Classification Research Group) and CRGCSTC (Cooperative Research Group on Chinese Soil Taxonomic Classification), 1991. Chinese Soil Taxonomic Classification (1st proposal). Science Press, Beijing, 112 pp.

Vandenberghe, J., An, Z.S., Nugteren, G., Lu, H.Y., Huissteden, K.V., 1997. New absolute time scale for the Quaternary climate in the Chinese loess region by grain-size analysis. Geology 25, 35–38.

Verosub, K.L., Fine, P., Singer, M.J., TenPas, J., 1993. Pedogenesis and paleoclimate: interpretation of the magnetic susceptibility record of Chinese loess-paleosol sequences. Geology 21, 1011–1014.

Williams, D.F., Thunell, R.C., Tappa, E., Rio, D., Raffi, I., 1988. Chronology of the Pleistocene oxygen isotope record: 0–1.88 m.y. B.P. Palaeogeography, Palaeoclimatology, Palaeoecology 64, 221–240.

Zhang, J.C., Lin, Z.G., 1987. Climate in China. Meteorology Press, Beijing, pp. 1–325 (in Chinese).

Zhu, H.J., 1985. Soil Geography of the World. China High Education Press, Beijing, 377 pp. (in Chinese).